Sky color near the horizon during a total solar eclipse

Stanley David Gedzelman

A theory for the color of the sky near the horizon for an observer in the umbral region of a total solar eclipse is presented. The model uses a Rayleigh scattering atmosphere, and the light reaching the observer is a beam of singly scattered sunlight, which, in turn, has suffered depletion by scattering in its passage from outside the shadow region. The model predicts both the red color observed in the lowest 8° of the sky for the total solar eclipse of 30 June 1973 and the enriched blue color of the sky at any elevation angle greater than the solar elevation angle. The model is also adapted to explain the reddening of the horizon sky observed during such times as when a dark cloud passes overhead or when the light from a large city is seen from the distance at night.

Introduction

During the day the sky normally appears blue, although the horizon is considerably whitened. Near sunrise and sunset, the horizon turns noticeably redder although the degree of redness varies dramatically from day to day depending mainly on the temperature and turbidity of the atmosphere. It is well known, for instance, that in the few years immediately following the explosion of Krakatoa, when the stratosphere was filled with volcanic dust, the sunsets throughout Europe were often brilliant red.

The cause of the redness near the horizon is explained rather simply.[1] When the sun is near the horizon the blue light in the direct solar beam that reaches the ground has been largely depleted because of Rayleigh scattering. The light scattered by the lower parts of the atmosphere will therefore have a greatly enhanced red contribution. In addition, at these times a greater percentage of scattered light reaching the observer comes from a considerable distance, and this light will be further deprived of its blue component by scattering as it approaches the observer.

Redness of the horizon can also be caused by a somewhat distinct set of phenomena. At night when one leaves the countryside and approaches a large city, a dirty orange color is quite often distinct over the city. The sky near the horizon will also turn a dirty orange when a thick layer of clouds, such as the leading edge of a squall line thunderstorm, has rolled over the observer. Finally, this reddening of the horizon is most dramatic during a total solar eclipse and has been noted by a number of observers since Halley. It is shown quite clearly in a beautiful picture taken just after the onset of totality of the eclipse of 15 February 1961 in extreme southeastern France when the sun was at an elevation angle of 9½°. This picture appears in the book, *The Beauty of the Universe,* and formed the initial inspiration for this paper, since I have never been fortunate enough to see a total solar eclipse.[2]

The cause of the reddening of the horizon for these situations is also quite straightforward and has also been known for a long time.[3] The area around the observer is illuminated almost entirely by distant parts of the atmosphere. As a light beam proceeds toward the observer, the blue light is preferentially scattered so that the beam is progressively reddened.

The scientific community has, by and large, overlooked the detailed behavior of the sky near the horizon during total solar eclipses and concentrated their efforts on obtaining measurements of the solar corona and of the sky near the zenith.[4–10] Important results concerning the behavior of the otherwise unobservable daytime upper atmosphere have also been obtained from various eclipse studies.[11]

Recently, Shaw provided the first detailed eclipse sky radiance data from zenith to horizon during the total solar eclipse of 30 June 1973.[12] The eclipse was observed at a point roughly 100 km from the edge of the shadow region during the height of totality, and the sun was at an elevation angle of 37°. Sky brightness decreased to $(1.3)\ (10)^{-4}$ of its normal value at wavelength $\lambda = 0.6\ \mu m$. In addition, Shaw also found that the blueness of the zenith sky was enhanced, while the sky near the horizon appeared reddish to a height of 8°. The enhanced blueness of the zenith sky during an eclipse is a universally agreed upon phenomenon. The horizon observation of the

The author is with the City College, CUNY, Department of Earth & Planetary Sciences, New York, New York 10031.

Received 13 June 1975.

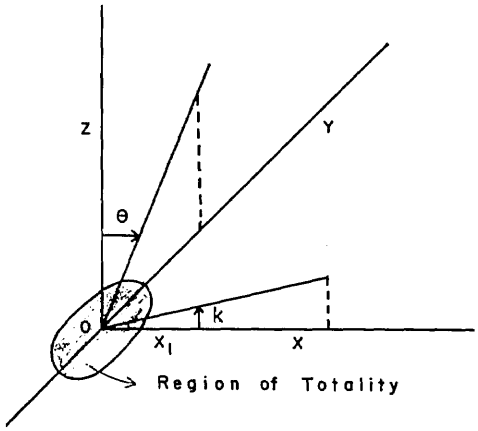

Fig. 1. Geometry of the eclipse. Shaded area is umbra. Observer looks in the x-z plane at elevation angle k. Sun is in the y-z plane at zenith angle θ. The shadow region is approximated by vertical walls.

30 June eclipse is consistent with the observation of Kennelly[4] who observed the rosy red color at 3° and also with the abovementioned photograph that showed a distinct orange-yellow color up to about 4°.

In view of the striking appearance of the horizon and the relatively simple qualitative explanation, it is quite surprising that no one has attempted to model the phenomenon mathematically until recently. In this paper the main features of the sky near the horizon during a total solar eclipse are reproduced by a simple model of a Rayleigh scattering atmosphere. The model is applied to the conditions of the 30 June 1973 eclipse observed by Shaw at Loiyengalani Oasis. It predicts both the distinct red sky color to an elevation angle of approximately 8° and the fact that for all elevation angles greater than the solar elevation angle, the sky is always bluer during an eclipse than it is otherwise.

We consider light entering the shadow region to be singly scattered sunlight and then allow this light to be depleted by scattering as it passes through the atmosphere to the observer. Second-order scattering is included only insofar as it causes depletion of the beam, and contributions to the beam from second and all higher orders of scattering are neglected entirely. This model is simpler than that proposed by Shaw. Comparisons of predictions of the model with observations of the 30 June eclipse indicate further that the contribution of singly scattered light to the beam is negligible above an elevation angle of approximately 20°. Our model is therefore valid only near the horizon, and all models purporting to describe the state of the zenith sky during an eclipse must include at least second-order scattering.

II. Model

An observer O is located in the center of the shadow region of the eclipse (or the cloud). We consider the light intensity, $B(\lambda, k, \theta)$, reaching the observer from outside the shadow region in a vertical plane perpendicular to the vertical plane containing the sun. We use cartesian coordinates (x, y, z) with z pointing vertically upward. The sun lies in the y-z plane at zenith angle θ, and the observer looks in the x-z plane at elevation angle k. The geometry of the situation is illustrated in Fig. 1. The boundary of the shadow region in the x-z plane is approximated by vertical walls located at a distance x_1 from the observer.

We consider the contribution to the brightness of a pencil of light to be due solely to singly scattered direct sunlight and therefore neglect any contribution due to reflection of sunlight from the earth's surface. We assume a Rayleigh scattering behavior for the turbid atmosphere so that the scattering coefficient per unit volume σ is given by

$$\sigma = K\rho/\lambda^4, \tag{1}$$

where K is a constant, ρ is the density of the air, and λ is the wavelength of the light. The contribution to the brightness of a pencil of light reaching the observer from a distance r is then given by

$$dB = F(r, k, \lambda, \theta)P \exp\left[\int_0^r \sigma\, dr\right] dr, \tag{2}$$

where $r = (x^2 + y^2)^{1/2}$, $F(r, k, \lambda, \theta)$ is the intensity of sunlight, and $P = \frac{3}{16}\pi(1 + \cos^2\theta \sin^2 k)$ is the angular factor for a Rayleigh scattering atmosphere.

Since we consider only small observation angles k in this article, we find that

$$\tan(k) = z/x = k = \sin(k) \text{ and } r = x. \tag{3}$$

It is now important to show that the combined effects of the sphericity of the earth and the refraction of the light passing through the atmosphere are small enough to be neglected for most purposes. A pencil of light that is horizontal at O will be found at a height h above the ground at a distance r from the observer where r is given by

$$x \cong r = \int_0^h \left[1 - \left(\frac{R}{R+h}\frac{n_0}{n}\right)^2\right]^{-1/2} dh. \tag{4}$$

R is the radius of the earth, and n is the index of refraction given by

$$n^2 = 1 + 2(n_0 - 1)\rho/\rho_0, \tag{5}$$

where $n_0 - 1 = (2.93)(10)^{-4}$ for white light.[13] We neglect the rather small dependence of n on wavelength. In all subsequent calculations we consider an isothermal atmosphere for reasons of mathematical simplicity so that

$$\rho = \rho_0 \exp(-h/H);\ H = R_g T/g. \tag{6}$$

H is the scale height of the atmosphere, and R_g, T, and g represent the ideal gas constant, the absolute temperature, and the acceleration of gravity, respectively. Since the light coming from distant parts of the sky is severely attenuated, we are mainly concerned with distances such that $r \ll R$. In addition, we assume that for $r \lesssim 200$ km, $h \ll H$. Using these inequalities together with Eqs. (5) and (6), the integral of Eq. (4) becomes approximately

$$h \cong \frac{x^2}{2}\left(R^{-1} - \frac{n_0 - 1}{H}\right). \quad (7)$$

The effect of atmospheric refraction is seen to offset partially the effect due to the sphericity of the earth. When $\rho_0 = 1.2$ kg m^{-3} and $H = (8)(10)^3$m (M.K.S. units are employed when not specified otherwise), we find that $h/H = 0.075$ when $x = 100$ km, and $h/H = 0.3$ when $x = 200$ km, so that the assumption that $h/H \ll 1$ is justified out to a distance of nearly 200 km, beyond which it is rapidly violated. This allows us to replace h with z in our calculations without introducing serious errors except when the sun is quite near the horizon.

We now wish to investigate some properties of the function $F(x, k, \lambda, \theta)$. Before encountering the atmosphere, the solar flux $F_0(\lambda)$ is a maximum for $\lambda = 0.47$ μm, while the extremes of the visible spectrum have slightly more than half of the value of $F_0(0.47$ μm). These variations are modeled by assuming the sun is a blackbody at a temperature of 5900 K. When the wavelength dependence of the solar flux is not included, the maximum brightness will occur at a wavelength closer to $\lambda = 0.47$ μm than is indicated by the calculations.

A second important cause of the variation of $F(x, k, \lambda, \theta)$ results from the fact that as the sun's beam passes through the atmosphere, scattering will preferentially reduce its blue component. The reddening that results is more severe at greater values of the solar zenith angle and at lower heights in the atmosphere. Except when the sun is quite near the horizon, we find that

$$F(x, k, \lambda, \theta) = F_0(\lambda) \exp\left[-\frac{KH\rho_0 \sec(\theta)}{\lambda^4} \exp(-kx/H)\right]. \quad (8)$$

Finally, during the eclipse the intensity of sunlight obviously increases with distance from the edge of the umbral region as a larger fraction of the sun is uncovered. We assume that the intensity of direct sunlight is proportional to the fraction of the area of the sun's disk not covered by the moon, that the apparent area of the sun and moon are equal, and that the sun is at an infinite distance. The fraction of the area of the sun that is uncovered is therefore given by

$$\frac{F_0(x, k, \lambda, \theta)}{F_0(\lambda)} = \frac{1}{\pi a^2}\left[\pi a^2 - 4\int_{\frac{x-x_1}{2}}^{a} (a^2 - y^2)^{1/2} dy\right], \quad (9)$$

where a is the radius of the penumbra of the moon. Since scattering severely depletes any light coming from great distances, the effective contribution to the brightness occurs only for $x \ll a$ so that Eq. (9) becomes approximately

$$\frac{F_0(x,k,\lambda,\theta)}{F_0(\lambda)} \cong \frac{2(x - x_1)}{\pi a}, \qquad x > x_1. \quad (10)$$

With all the foregoing approximations and assumptions, the expression for the brightness of an isothermal atmosphere becomes

$$B(k, \lambda, \theta) = F_0(\lambda) p \frac{K\rho_0}{\lambda^4} \int_{x_1}^{\infty} Q \exp\left(-\frac{kx}{H} - \frac{K\rho_0 H}{k\lambda^4}\left\{1 - [1 - \text{ksec}(\theta)] \cdot \exp(-kx/H)\right\}\right) dx, \quad (11)$$

where

$$Q = \frac{2(x - x_1)}{\pi a} \text{ during an eclipse,}$$

$$Q = 1 \qquad \text{otherwise.}$$

III. Analysis of the Model

In this section we analyze the behavior of the sky brightness and color as given by Eq. (11). In the numerical calculations that follow we assume that $a = (3)(10)^6$ m, $H = (8)(10)^3$ m, and $\rho = 1.2$ kg m^{-3}. For the eclipse we choose $x_1 = 100$ km, and unless specified otherwise, $\theta = 53°$. We also use $K_t = 2.5K_r = (2.08)(10)^{-30}$ m^6 kg^{-1}, where K_t is the total contribution to Rayleigh scattering when the role of aerosols is included. The values of K_t, x_1, and θ are based on the measurements of Shaw at the site of the 30 June 1973 eclipse. It should be noted that for most other solar eclipses, x_1 will generally be smaller.

At the horizon, $k = 0$, and when Eq. (11) is integrated we obtain

$$B_e(0, \lambda, \theta) = F_0(\lambda) p \frac{2\lambda^4}{\pi a K\rho_0} \exp\left\{-\frac{K\rho_0}{\lambda^4}[x_1 + H\sec(\theta)]\right\}. \quad (12)$$

From this point on, the subscript e will indicate eclipse conditions, n will indicate normal conditions, and c will indicate a shadow imposed by a dark cloud. When nothing obscures the sun, x_1 becomes zero.

The factor, $2\lambda^4/\pi a K\rho_0$ is peculiar to the geometry of the eclipse and is due to the fact that the intensity of sunlight increases in a roughly linear manner with distance from the edge of the umbral region. The inclusion of this factor leads to a significant increase in the redness of the horizon sky because the bulk of the scattered light reaching the observer is coming from places some distance removed from the edge of the region of totality. The longer effective pathlength for the light results in a considerable reduction of the contribution of the blue end of the spectrum.

Above the horizon the integral of the right-hand side of Eq. (11) is given by

$$B_e(k, \lambda, \theta) = F_0(\lambda) p \frac{H^2 K\rho_0 2}{k^2\lambda^4 \pi a} \exp(-K\rho_0 H/k\lambda^4) \exp(-kx_1/H) \times \left(1 + \sum_{n=2}^{\infty} \frac{\exp[-kx_1(n-1)/H]\left\{\frac{K\rho_0 H}{k\lambda^4}[1 - \text{ksec}(\theta)]\right\}^{n-1}}{(n)(n!)}\right). \quad (13)$$

We have found that for $k \geq 0.10$ and $x_1 = 100$ km, all terms under the summation sign in Eq. (13) can be neglected for all λ for which B_e is significant. This conclusion is also obtained by noticing that for sufficiently large k and x_1 in Eq. (11) that exp $(-kx_1/H)K\rho_0 H/k\lambda^4 \ll 1$. One feature of interest that then emerges is that for large enough k, B_e is vir-

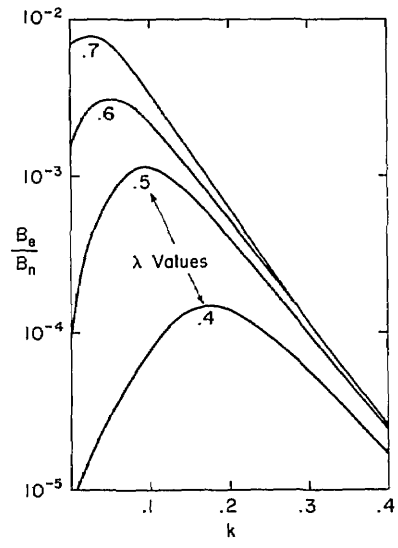

Fig. 2. Ratio of brightness during eclipse with x_1 = 100 km to brightness during normal times as a function of observer's elevation angle for various wavelengths. In all figures, λ is given in terms of microns.

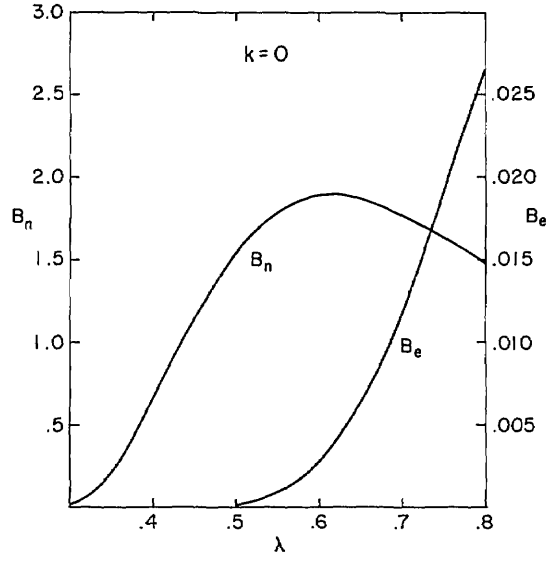

Fig. 3. Brightness of the sky at the horizon seen by observer during eclipse and noneclipse conditions as a function of wavelength.

tually independent of the solar zenith angle. This results from the fact that the pencil of scattered light is found at a considerable height by the time it emerges from the umbral region, and therefore even when the sun is rather low in the sky, the direct solar beam has been only slightly depleted in its passage through the atmosphere up to that point.

Under noneclipse conditions, the expression for the brightness becomes

$$B_n(k, \lambda, \theta) = F_0(\lambda)P[1 - k\sec(\theta)]^{-1} \times \left\{\exp[-K\rho_0 H \sec(\theta)/\lambda^4] - \exp\left(-\frac{K\rho_0 H}{k\lambda^4}\right)\right\}. \quad (14)$$

Although Eqs. (13) and (14) appear to be rather complicated, they contain much useful information concerning the brightness and color of the sky.

Shaw found that sky brightness during the height of totality at λ = 0.6 μm was reduced to $1.3(10)^{-4}$ of the normal sky value. Figure 2 contains a plot of B_e/B_n at λ = 0.6 μm as a function of the elevation angle k. Near the horizon, B_e/B_n far exceeds $(1.3)(10)^{-4}$. Although a good part of this excess is to be expected because of the relative enhancement of the longer wavelengths at the horizon during the eclipse, this ratio is still overestimated because of neglect of the curvature of the earth. This feature will be explained in more detail a little later in the paper. Beyond k = 0.25, B_e/B_n drops off rapidly with increasing k for all visible wavelengths. This is an indication that primary scattering plays a negligible role in the brightness of the eclipse sky much above the horizon (i.e., $k \gtrsim 0.4$). An accurate model of the sky brightness and color near the zenith must therefore include at least second-order scattering. Despite this drawback, B_e/B_n gives a crude estimate of darkening near the horizon during an eclipse.

Equations (12), (13), and (14) can also be used to show some color features of the sky. Figure 3 compares B_n with B_e at elevation angle k = 0. Both curves show that the light coming from the horizon has a tendency to be dominated by the longer wavelengths, but while there is no sharp maximum for the noneclipse sky, the deep red color of the eclipse sky is immediately apparent. It is expected that during normal times the effects due to second-order scattering will reduce the redness of the horizon indicated by Fig. 3.

Figures 4 and 5 also compare B_n with B_e (although without the factor P) for elevation angles of k = 0.1 and k = 0.2, respectively. The eclipse sky is redder than the normal sky for these graphs although the color difference becomes less marked with increasing k. Another important feature that emerges is the fact that at k = 0.1 (elevation angle = 6°), the eclipse sky is still red although by k = 0.2 (elevation angle =

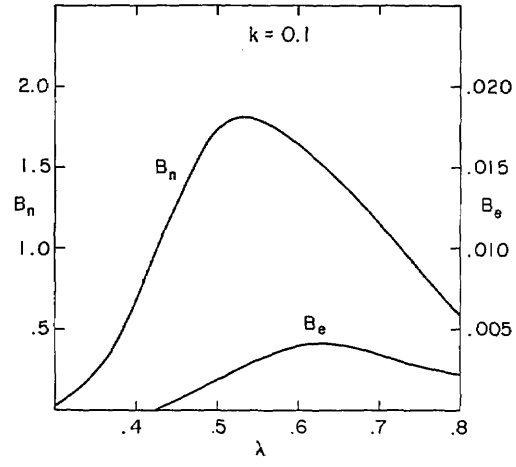

Fig. 4. Same as Fig. 3 but for k = 0.10.

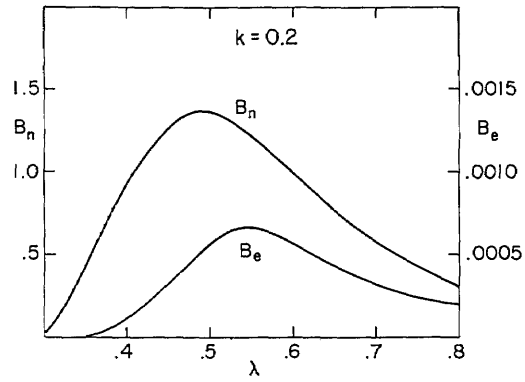

Fig. 5. Same as Fig. 3 but for $k = 0.20$.

11.5°) the eclipse sky probably appears yellow-green. Interpolation between Figs. 4 and 5 indicates that the sky has an orange color up to 8° or 9° above the horizon, and this agrees quite closely with the visual observations of Shaw. One can also see from Fig. 5 that the normal blue color of the sky under noneclipse conditions is beginning to emerge.

Much physical insight can be obtained by examining the integrand of Eq. (11). Neglecting the variation of intensity of sunlight due to wavelength $F_0(\lambda)$ we find that the maximum contribution to dB occurs at the wavelength given by

$$\lambda_{max}^4 = \frac{K\rho_0 H}{k}\{1 - \exp(-kx/H)[1 - k\sec(\theta)]\}. \quad (15)$$

It is apparent that the sky reddens with increasing turbidity and increasing solar zenith angle. Eclipses, like sunsets, will therefore appear more dramatic if the air is somewhat polluted. The sky reddens with increased θ because the direct sunlight must then pass through an increased thickness of atmosphere before reaching a given height, and as a result the blue component of direct sunlight becomes rapidly depleted by scattering. When light from this depleted sunbeam is in turn scattered toward the observer, it is seen to be enriched in red. For small k, the sky reddens as the horizon is approached because of the longer effective path.

The reason that the sky near the horizon is redder during an eclipse is due to the fact that the effective light reaching the observer comes from a greater distance during an eclipse than during normal times. Equation (15) shows that λ_{max} increases with increasing x so long as $k\sec(\theta) < 1$. Recall that x represents the distance at which sunlight enters the scattered beam. Light coming from larger x has a larger optical path to traverse through the atmosphere so long as $k\sec(\theta) < 1$, and therefore the blue end of the spectrum is preferentially depleted by scattering.

On the other hand, when $k\sec(\theta) > 1$, light coming from a greater value of x has a smaller optical path than light coming from smaller values of x. This corresponds to the situation when the observation angle is greater than the solar elevation angle. Figure 6 illustrates this point, and we see that path 4 is effectively shorter and hence bluer than the other paths. In this case the blue contribution to the brightness increases with x and leads to the conclusion that the eclipse sky should be bluer above the solar elevation angle than the normal sky.

The conclusion that the eclipse sky is always bluer than the noneclipse sky above the solar elevation angle is consistent with the observations that during an eclipse the blueness of the zenith is enhanced. Quantitative agreement, however, is not to be expected on this point for our model because of the fact that primary scattering becomes negligible much above the horizon. Therefore, it cannot be asserted than Eq. (15) contains an explanation for the increased blueness of the zenith sky during an eclipse, although a similar geometrical picture for the higher orders of scattering is likely.

Figures 7 and 8 show the integrand of Eq. (11) at $\lambda = 0.5\ \mu m$ as a function of x during eclipse and noneclipse conditions, respectively, for several values of k. During noneclipse conditions the contribution to the brightness decreases sharply beyond x_1. During

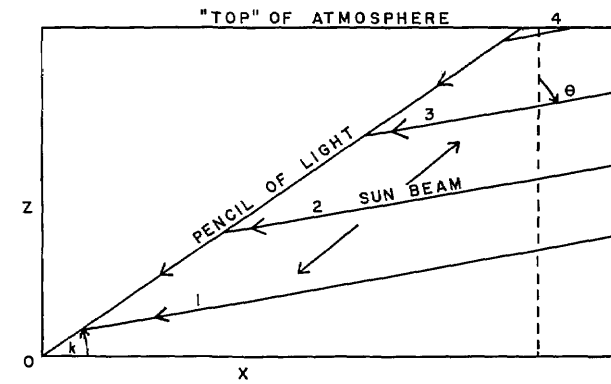

Fig. 6. Schematic diagram for pathlength of light through the atmosphere when the solar elevation angle is less than the observation elevation angle. Notice that pathlength 1 > 2 > 3 > 4.

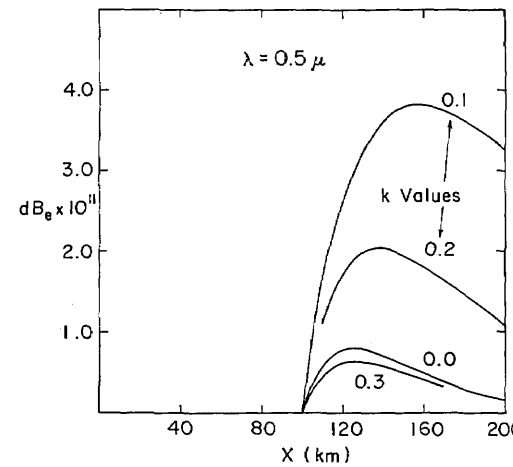

Fig. 7. Contribution to the brightness as a function of distance x along the scattered beam for $\lambda = 0.5\ \mu m$ during an eclipse.

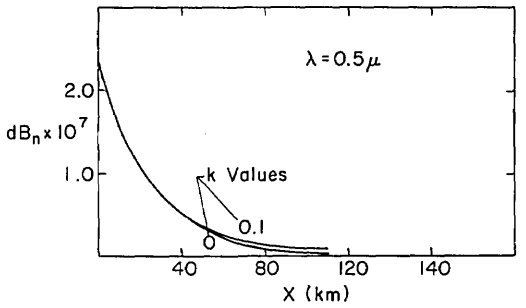

Fig. 8. Same as Fig. 7 but during noneclipse conditions.

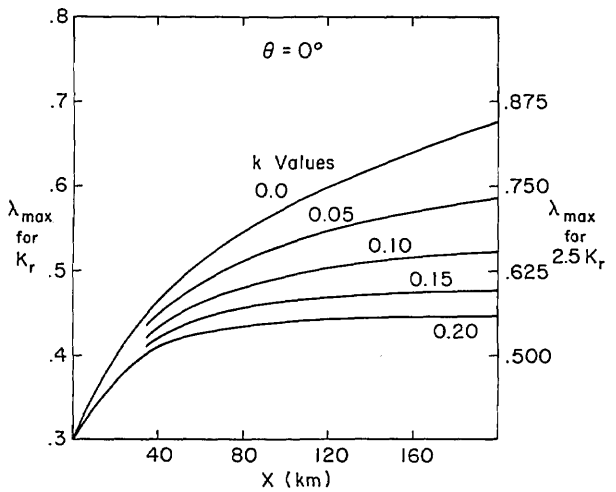

Fig. 9. Wavelength of maximum intensity, neglecting the factor $F_0(\lambda)$ as a function of x with $\theta = 0°$.

eclipse conditions, the maximum value of the integrand arises from a distance x_{max} given by

$$1 = (x_{max} - x_1)\frac{k}{H}\left\{1 + \frac{K\rho_0 H}{k\lambda^4}[1 - k\sec(\theta)]\exp(-kx_{max}/H)\right\}. \quad (16)$$

At the horizon, this transcendental equation reduces to

$$x_{max} = x_1 + (\lambda^4/k\rho_0), \quad (17)$$

which for $\lambda = 0.5$ μm indicates that the maximum contribution to the brightness arises from about 25 km beyond the umbral region. For sufficiently large k, Eq. (16) reduces to

$$x_{max} = x_1 + (H/k), \quad (18)$$

which is independent of wavelength. For $k = 0.2$, the maximum contribution to the brightness arises from 40 km beyond the umbral region.

Several points remain to be cleared up. The fact that we have overestimated the ratio B_e/B_n is, as already mentioned, due to the neglect of the curvature of the earth. During eclipse conditions a considerable contribution to the integral arises from parts of the atmosphere for which $x \geq 200$ km. It is this part of the integral that is considerably overestimated by the neglect of the earth's curvature. In actuality, far less light is scattered into the beam beyond 200 km because of the increased height and reduced density. On the other hand, depletion of the light coming from great distances is affected far less by the curvature term since, except when $k = 0$, the depletion is largest at small values of x where the curvature term is negligible. As a result, B_e is considerably overestimated by Eq. (11).

During noneclipse conditions, virtually all the light reaching the observer comes from within 100 km so that the expression for B_n is virtually unaffected by neglecting the curvature term. The ratio of B_e/B_n is therefore spuriously enlarged by neglecting the curvature of the earth.

This may lead one to question the accuracy of Eq. (11) for determining the color of the eclipse sky as a function of k. Nevertheless, we find in this case that Eq. (11) gives quite reliable results. Figure 7 shows that even when the curvature effects are neglected, the bulk of light reaching the observer comes from a region of the order of 50 km from the edge of the umbral region. Since the effect of curvature is small for $x \lesssim 200$ km, Eq. (15) closely estimates the wavelength that yields the maximum contribution to the brightness for a particular set of (x, k, θ) when the variation of solar intensity with wavelength is neglected. The results of Eq. (15) are plotted in Figs. 9 and 10. Except right at the horizon, there is little change in λ_{max} much beyond 100 km. The overestimate of the integrand of Eq. (11) for $x \gtrsim 200$ km therefore contains almost no color bias. When the contribution to B_e beyond 200 km does include the curvature, the former is small enough so that it has negligible effect on the color of the sky.

Use of the fact that during an eclipse the major contribution to the brightness comes from about 50 km outside the umbral region combined with use of Figs. 9 and 10 can help tell to what height the sky should appear red for other eclipses. Increasing x_1 above 100 km will not add significantly to the height at which the red color is to be found since λ_{max} levels

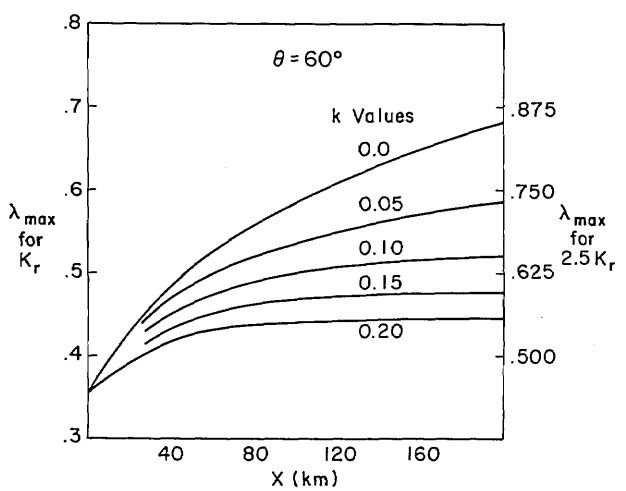

Fig. 10. Same as Fig. 9 but with $\theta = 60°$.

off after 150 km. Generally, during an eclipse the observer is less than 100 km from the edge of the shadow region. If, for instance, the edge of the shadow region is 40 km from the observer (as was the case during the May 1900 eclipse), the sky should appear orange to a height of 6° at the height of totality if $K_t = 2.5K_r$.

At the horizon Eq. (15) seriously overestimates λ_{max}^4 only as $x \to \infty$. When the curvature of the earth is included, we find that

$$\lambda_{max}^4 \longrightarrow K\rho_0\left[\frac{\pi H}{2\left(\frac{1}{R} - \frac{n_0 - 1}{H}\right)}\right]^{1/2} \quad \text{as} \quad x \longrightarrow \infty \quad (19)$$

or $\lambda_{max} \to 0.89\ \mu m$ as $x \to \infty$. This, however, does not in any way affect the conclusion that during an eclipse the horizon appears red.

When we consider the horizon sky color during a time when dark clouds have passed overhead, we can assume that essentially no light penetrates through the cloud.[13] Accurate measurements of light penetrating large, thick cumulonimbus clouds do not exist, but we can confidently assert that the intensity of light penetrating the cloud base is less than 1% of the incident sunlight. For this reason and for the sake of simplicity, we therefore neglect all transmission of sunlight through the cloud. Once we leave the shadow region, we assume that the sunlight immediately switches on to full intensity. Equation (11) then integrates to

$$B_c = F_0(\lambda)P \exp\left(\frac{-k\rho_0 H}{k\lambda^4}\right)[1 - k\sec(\theta)]^{-1} \times \left(\exp\left\{\frac{k\rho_0 H}{k\lambda^4}[1 - k\sec(\theta)]\exp(-kx_1/H)\right\} - 1\right). \quad (20)$$

At the horizon, $B_c(0, \lambda, \theta)$ resembles B_e but lacks the geometrical factor $2\lambda^4/\pi a K\rho_0$. At the horizon the eclipse sky is redder than the cloud covered sky. This is due to the fact that in the case of the eclipse the effective light is coming from some distance beyond the edge of the shadow region, and the blue light is experiencing extra depletion by scattering. By the geometrical arguments given before, we therefore expect that the eclipse sky will be redder than the cloud covered sky at all heights below the solar elevation angle and bluer at all heights above the solar elevation angle.

The cloud covered sky should appear noticeably red at the horizon whenever $[H \sec(\theta) + x_1]$ is large enough, i.e., if either the sun is low enough in the sky or if the shadow region is sufficiently wide. In addition, second-order scattering effects, which reduce the reddening of the horizon sky under clear weather, will naturally be less effective when a dark cloud is overhead.

I gratefully acknowledge the careful and informative review given by Glenn Shaw whose comments led to a number of important changes in this paper.

The author is also affiliated with the CUNY Institute of Marine and Atmospheric Sciences

References

1. W. J. Humphreys, *Physics of the Air* (McGraw Hill, New York, 1940).
2. H. Rohr, *The Beauty of the Universe* (Viking, New York, 1972).
3. M. Minnaert, *Light and Color in the Open Air* (Dover, New York, 1954).
4. S. Silverman and E. Mullen, *Sky Brightness During Eclipses*, AFCRL-TR-74-0363 (1974).
5. W. E. Sharp, J. Lloyd, and S. Silverman, Appl. Opt. **5**, 787 (1966).
6. B. S. Dandekar, Appl. Opt. **7**, 705 (1968).
7. W. E. Sharp, S. Silverman, and J. Lloyd, Appl. Opt. **10**, 1207 (1971).
8. D. A. Velasquez, Appl. Opt. **10**, 1211 (1971).
9. J. Lloyd and S. Silverman, Appl. Opt. **10**, 1215 (1971).
10. B. Dandekar and J. P. Turtle, Appl. Opt. **10**, 1220 (1971).
11. W. Benyon and G. Brown, Eds., *Solar Eclipses and the Ionosphere* (Pergamon, London, 1956).
12. G. Shaw, Appl. Opt. **14**, 388 (1975).
13. K. Kondratyev, *Radiation in the Atmosphere* (Academic, New York, 1969).

RESEARCH SCHOOL OF PHYSICAL SCIENCES
THE AUSTRALIAN NATIONAL UNIVERSITY
CANBERRA, A.C.T., 2600 AUSTRALIA

Allan W. Snyder has been made a Professorial Fellow of the Institute of Advanced Studies, Department of Applied Mathematics.

Professor Snyder will continue directing activities in Vision Research, particularly on the structure and function of visual photoreceptors and optical physics with emphasis on the theory of optical waveguides.